Lab on a Chip

PAPER

View Article Online
View Journal | View Issue

Cite this: *Lab Chip*, 2022, **22**, 1748

Portable sample processing for molecular assays: application to Zika virus diagnostics†

Tanya Narahari,‡[ab] Joshua Dahmer,‡[a] Alexandros Sklavounos, ‡[ab] Taehyeong Kim, ‡[ab] Monika Satkauskas,‡[a] Ioana Clotea,[a] Man Ho,[ab] Julian Lamanna,[ab] Christopher Dixon, [a] Darius G. Rackus, §[ac] Severino Jefferson Ribeiro da Silva, ¶[d] Lindomar Pena,[d] Keith Pardee[ce] and Aaron R. Wheeler *[abf]

This paper introduces a digital microfluidic (DMF) platform for portable, automated, and integrated Zika viral RNA extraction and amplification. The platform features reconfigurable DMF cartridges offering a closed, humidified environment for sample processing at elevated temperatures, as well as programmable control instrumentation with a novel thermal cycling unit regulated using a proportional integral derivative (PID) feedback loop. The system operates on 12 V DC power, which can be supplied by rechargeable battery packs for remote testing. The DMF system was optimized for an RNA processing pipeline consisting of the following steps: 1) magnetic-bead based RNA extraction from lysed plasma samples, 2) RNA clean-up, and 3) integrated, isothermal amplification of Zika RNA. The DMF pipeline was coupled to a paper-based, colorimetric cell-free protein expression assay for amplified Zika RNA mediated by toehold switch-based sensors. Blinded laboratory evaluation of Zika RNA spiked in human plasma yielded a sensitivity and specificity of 100% and 75% respectively. The platform was then transported to Recife, Brazil for evaluation with infectious Zika viruses, which were detected at the 100 PFU mL^{-1} level from a 5 μL sample (equivalent to an RT-qPCR cycle threshold value of 32.0), demonstrating its potential as a sample processing platform for miniaturized diagnostic testing.

Received 26th November 2021,
Accepted 18th March 2022

DOI: 10.1039/d1lc01068a

rsc.li/loc

Introduction

Recent disease outbreaks around the world, including the 2015–16 Zika outbreak in South America[1] and the ongoing SARS-CoV-2 pandemic[2] have underscored the need for portable, point-of-care platforms that can extract and quantify viral RNA from patient samples, and help distribute the diagnostic burden on the healthcare system. Automated platforms are of particular interest as most extraction and diagnostic techniques are labour intensive, often requiring a series of 'wash' steps performed in an aseptic, nuclease-free environment, that can make remote monitoring and decentralized testing especially challenging. While portable diagnostic sensors have (with good reason) attracted great attention, the pre-processing steps required upstream of the sensor are often ignored, leading some[3] to label them the "forgotten beginning" of portable diagnostics.

Microfluidic devices have a proven track-record in automated liquid handling of the kind required for decentralized testing. For example, there are many reports[4–12] of low-cost and portable paper and fabric-based microfluidic platforms which can serve as self-actuated, pump-free devices for nucleic acid testing. Though extremely affordable and easily disseminated for large scale screening purposes, these platforms typically require the user to manually pre-process the samples prior to analysis, and are often not capable of liquid-phase extraction and amplification.[13] Microfluidic systems relying on enclosed microchannels such as continuous flow-through q-PCR,[14–16]

[a] *Department of Chemistry, University of Toronto, 80 St. George Street, Toronto, Ontario, M5S 3H6, Canada. E-mail: aaron.wheeler@utoronto.ca*
[b] *Donnelly Centre for Cellular and Biomolecular Research, University of Toronto, 160 College Street, Toronto, Ontario, M5S 3E1, Canada*
[c] *Leslie Dan Faculty of Pharmacy, University of Toronto, 144 College Street, Toronto, Ontario, M5S 3M2, Canada*
[d] *Department of Virology, Aggeu Magalhães Institute (IAM), Oswaldo Cruz Institute (FIOCRUZ Pernambuco), Av. Professor Moraes Rego, s/n – Cidade Universitária, Recife, PE, CEP 50.740-465, Brazil*
[e] *Department of Mechanical and Industrial Engineering, University of Toronto, Toronto, Ontario, M5S 3G8 Canada*
[f] *Institute for Biomedical Engineering, University of Toronto, 164 College Street, Toronto, Ontario, M5S 3G9, Canada*

† Electronic supplementary information (ESI) available. See DOI: **https://doi.org/10.1039/d1lc01068a**

‡ Equal contributors.

§ Current address: Department of Chemistry and Biology, Ryerson University, 350 Victoria St., Toronto, Ontario, Canada M5B 2K3.
¶ Current address: Leslie Dan Faculty of Pharmacy, University of Toronto, 144 College Street, Toronto, Ontario, M5S 3M2, Canada.

rotary devices,[17,18] droplet-based systems,[19,20] and integrated systems for extraction and amplification[21–25] offer a liquid-phase alternative to paper-based systems. However, integrated channel-based systems require complex, custom architecture and external instrumentation including pumps, interconnects, and valves, with specific, design-mediated device functions that cannot be changed after design and manufacture.

Digital microfluidics (DMF) is an alternative to the techniques described above, in which liquids are manipulated as discrete droplets using electrostatic forces.[26] Specifically, droplets in DMF devices are actuated by applying electric potentials to an array of insulated electrodes in an integrated glass or plastic cartridge. Unlike other microfluidic technologies, a generic device design can be used to perform combinations of unit operations such as droplet metering, splitting, merging, and mixing that can be selected on-the-fly (*i.e.*, not pre-determined by device geometry). Protocols are reconfigurable and programmable *via* open-source software,[27] allowing serological immunoassays[28–30] and molecular tests[31–36] to be adapted to a universal hardware platform. In prior work, we developed and evaluated portable DMF-ELISA systems for measles and rubella sero-surveillance in remote communities in Kenya[28] and the Democratic Republic of Congo.[29,30] These platforms were built using open-source hardware, and the latter iteration[29,30] was operated on 12 V DC power supplied by rechargeable battery packs, allowing outdoor use, and featured a motorized, magnetic stage to manipulate magnetic beads that served as a solid phase for analyte capture. This paper describes a new generation of this system, applied to a very different application – the integrated extraction and isothermal amplification of viral RNA from serum samples, upstream of a colorimetric assay for amplified Zika RNA.

The cutting-edge assay featured here relies on Zika virus-specific toehold-switch riboregulators and cell-free paper-based colorimetric detection, a concept that was established in previous work by Pardee *et al.*[37,38] The switch contains a sequence complementary to a portion of the Zika genome, ligated to a riboregulator sequence necessary for protein translation, which is in turn ligated to a *lacZ* reporter, all bound in a hairpin loop structure. In the presence of Zika RNA, the switch linearizes, causing the expression of β-galactosidase and leading to a colorimetric response proportionate to the amount of Zika RNA present in the sample. This system was recently optimized for fieldwork and was validated in combination with a novel custom plate reader device, called PLUM[39] (portable, low-cost, user-friendly, multimode), which features temperature control, and optical monitoring of up to 384 simultaneous reactions and onboard data analysis. These innovations,[37–39] which are focused on assay development and implementation, are tremendously important. Here we tackle a different problem – the need for substantial sample processing prior to analysis.

To address the need for automated sample processing, we built a new DMF sample processing platform known as the "Zed Box" for Zika virus nucleic acid testing. In contrast to previously reported DMF systems for nucleic acid amplification,[31–36] the new system allows for droplet-in-air amplification using humidified cartridges that do not require oil fillers[32,35] or solvent injection[36] to counter droplet evaporation at elevated temperatures. The system is therefore straightforward to use and amenable to implementation in real-world settings where users may lack experience with operating microfluidic devices. The workflow introduced here (Fig. 1A) involves five major steps: 1) sample lysis and reversible RNA capture on magnetic beads, 2) RNA extraction, 3) RNA clean-up, 4) isothermal amplification of Zika RNA by nucleic acid sequence based amplification[40] (NASBA), and 5) detection using the aforementioned toehold switch-based Zika virus sensors.[37–39] In this scheme, we describe integration of steps 2–4 (Fig. 1B) on the DMF sample processing platform, while step 5 is performed separately, but future DMF iterations might be developed to include the complete pipeline, from sample to analysis.

Here, we describe DMF cartridges, workflow integration, design and validation of control hardware and thermal cycling module, and workflow evaluation with simulated samples containing Zika RNA. Finally, we report the testing of infectious, lab-grown Zika virus in Recife, Pernambuco, Brazil, as demonstration of proof of concept for the platform's functionality and portability. We propose that the simple user interface and low barrier to field-implementation described here makes this system an attractive new tool for automated nucleic-acid testing for disease diagnosis.

Materials and methods

Unless otherwise stated, reagents were purchased from Millipore Sigma (Oakville, ON), and electronic components were purchased from Digi-Key. Tetronic 90R4 (BASF Corp., Germany) was generously donated by Brenntag Canada (Toronto, ON). Chromium and photoresist-coated glass slides (3 in × 3 in) used to fabricate DMF bottom plates were purchased from Telic Company (Valencia, CA). Acrylic and ITO-coated polyethylene sheets (PET-ITO) used to fabricate DMF top plates were purchased from McMaster-Carr (Princeton, NJ), and Memcon (Stevensville, MI) respectively. PCR plate sealing film (Microseal 'B') was purchased from Biorad (Mississauga, ON). Medical grade, pressure sensitive adhesive tape (AR Care® 90106NB and 7761-19) for DMF gaskets and top plates was graciously donated by Adhesives Research (Glen Rock, PA). Absorbent pads and humidification pads were cut from Wypall® paper towels from Kimberly Clark Corporation (Neenah, WI). FluoroPel PFC 1101V and PFC 110 solvent were purchased from Cytonics, LLC (Beltsville, MD). Murine RNase inhibitor (40 U mL^{-1}) and *in vitro* (cell free) protein synthesis kits (PURExpress®) were purchased from New England Biolabs (Ipswich, MA). RNA extraction reagents were adapted from the Genesig Easy® DNA/RNA extraction kit by Primerdesign (Camberley, UK). Nucleic acid sequence based amplification (NASBA) kits were purchased from Life Sciences Advanced Technologies (St. Petersburg, FL), and NASBA forward and

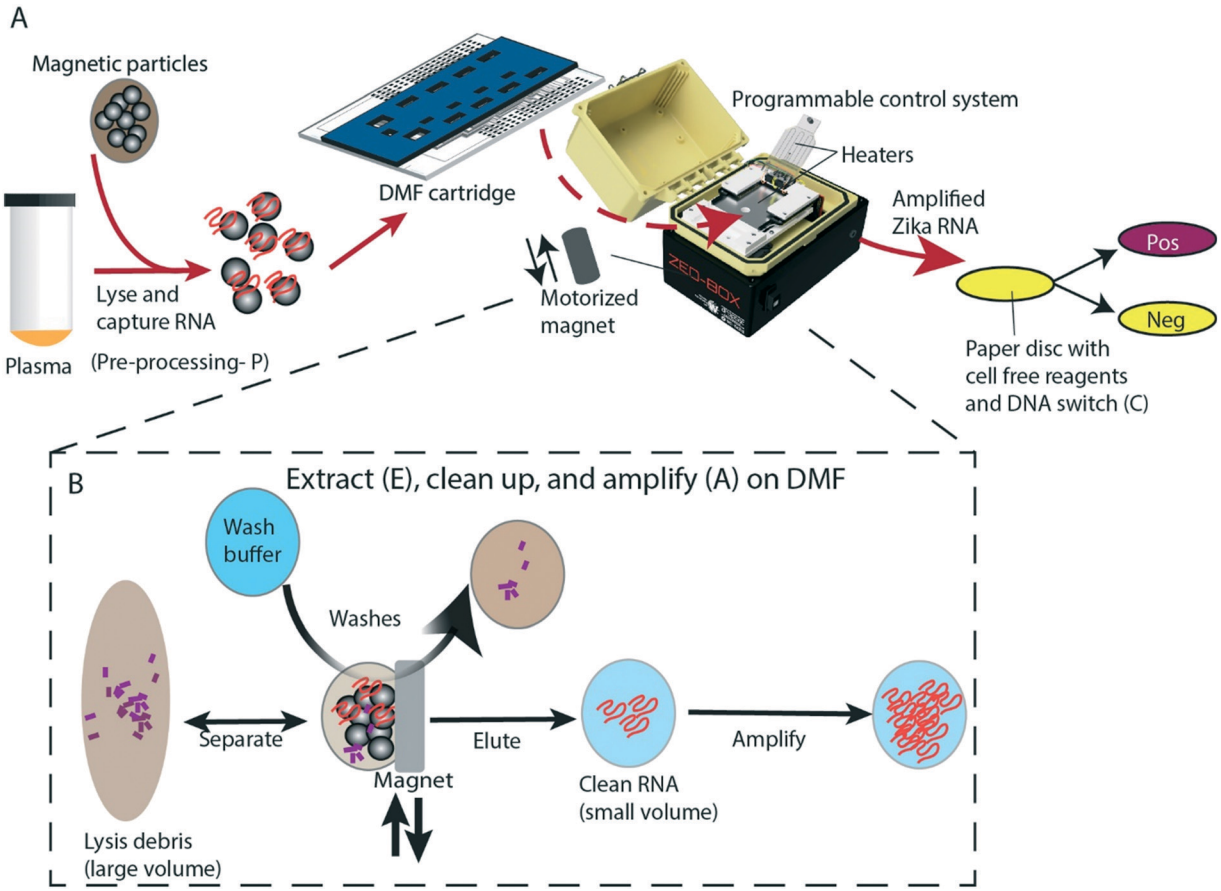

Fig. 1 Schematics of the DMF Zika diagnostic sample processing system and assay workflow. A) A sample of plasma (orange) potentially containing virus is lysed (denoted pre-processing or 'P'), and RNA (red traces) is reversibly captured on magnetic beads (gray circles). The magnetic beads are then processed on DMF using the Zed Box, which includes a motorized magnet and built-in thermal cycling system, which enables automated RNA extraction and cleanup (denoted 'E'), as well as Zika RNA amplification (denoted 'A') *via* a programmable protocol. The amplified product is then assayed using a one-pot, paper-based, colorimetric, cell free protein expression system[20] (denoted 'C') revealing a colour change from yellow (negative) to deep red (positive). B) In the Zed Box, sample matrix and lysis debris (purple) are separated from captured RNA (red traces on gray beads) *via* the built-in magnet (gray rectangle), which can be raised or lowered to pellet, resuspend, and wash the beads as many times as required in an automated fashion (black arrows). Purified RNA (red traces) is eluted and then isothermally amplified.

reverse primers were sourced from Eurofins Genomics (Louisville, KY) based on primer designs established in prior work.[38] Healthy human plasma was purchased from Innovative Research (Novi, MI).

DMF cartridge design and manufacture

All cartridge components were designed using AutoCAD™ software. Bottom plates were manufactured from 3 in × 3 in chromium-coated glass substrates at the Toronto Nanofabrication Center (TNFC) as described previously[27] *via* UV photolithography and wet etching. The electrode array included 58 square interdigitated driving electrodes (2.8 mm × 2.8 mm), 5 loading electrodes (four measuring 2.8 mm × 5.6 mm, and one measuring 5 mm × 4 mm), 8 buffer reservoir electrodes (11 mm × 6.5 mm), 10 dispensing electrodes (2.8 mm × 5.6 mm), and 3 extraction lane reservoir electrodes (7 mm × 6.4 mm), each connected by a conductive trace to a contact pad on the edges, laid out as indicated in Fig. S1A.† After formation, bottom plates were coated with an 8 μm layer of parylene C *via* vapor deposition, and then spin-coated with a fluorocarbon resin (2% w/w FluoroPel PFC 1101V in PFC110) at 2000 rpm for 30 s. Coated bottom plates were post-baked in a dry oven at 120 °C for 10 min.

Top plates were composed of a rigid, visually transparent acrylic substrate (1.5 mm thick) interfaced with a flexible PET-ITO electrical grounding layer (MITO-60-125, 60 Ω sq. $in.^{-1}$, 125 μm thick). To fabricate each top plate, acrylic substrates were laser-cut using a Hobby Series Full Spectrum, 40 W CO_2 benchtop laser cutter (at power, speed, and vector current set to 100%, 30%, and 100% respectively) into 8 cm × 5 cm pieces, punctuated with three kinds of rectangular windows (through-holes), including eight ~5.5 mm × 4 mm reservoir windows, four ~3 mm × 4 mm and one ~5 mm × 2.5 mm loading window, and two 7 mm × 6.5 mm extraction windows. The windows were spaced such that when mounted above a bottom plate, they aligned with the reservoir

electrodes, the loading electrodes, and the extraction lane reservoir electrodes (denoted waste reservoir, sample reservoir, and buffer reservoir), respectively. PET-ITO parts were lasercut (at power, speed, and vector current set to 30%, 30%, and 35% respectively) to the same outer dimensions as the acrylic pieces, punctuated with identically spaced windows. Each reservoir window in the PET-ITO substrate was 2 mm narrower than its analogue in the acrylic piece (Fig. S1B†) – *e.g.*, the reservoir windows in the PET-ITO piece were ~5.5 mm × 2 mm. The "outer" 2 mm adjacent to each window in the PET-ITO piece (relative to the device) was termed the 'flap' and its edges were scored and creased using a laser cutter (at power, speed and vector current set to 50%, 5%, and 35% respectively), such that the flap could bend up or down. A piece of double-sided adhesive tape (ARCare® 90106NB) with each adhesive side ("lower" and "upper") protected by a liner, was used to join the acrylic and PET-ITO parts. Pieces of tape were prepared by cutting the adhesive sheet to the dimensions of the acrylic piece using a Silhouette Cameo2™ craft cutter (blade length, speed and

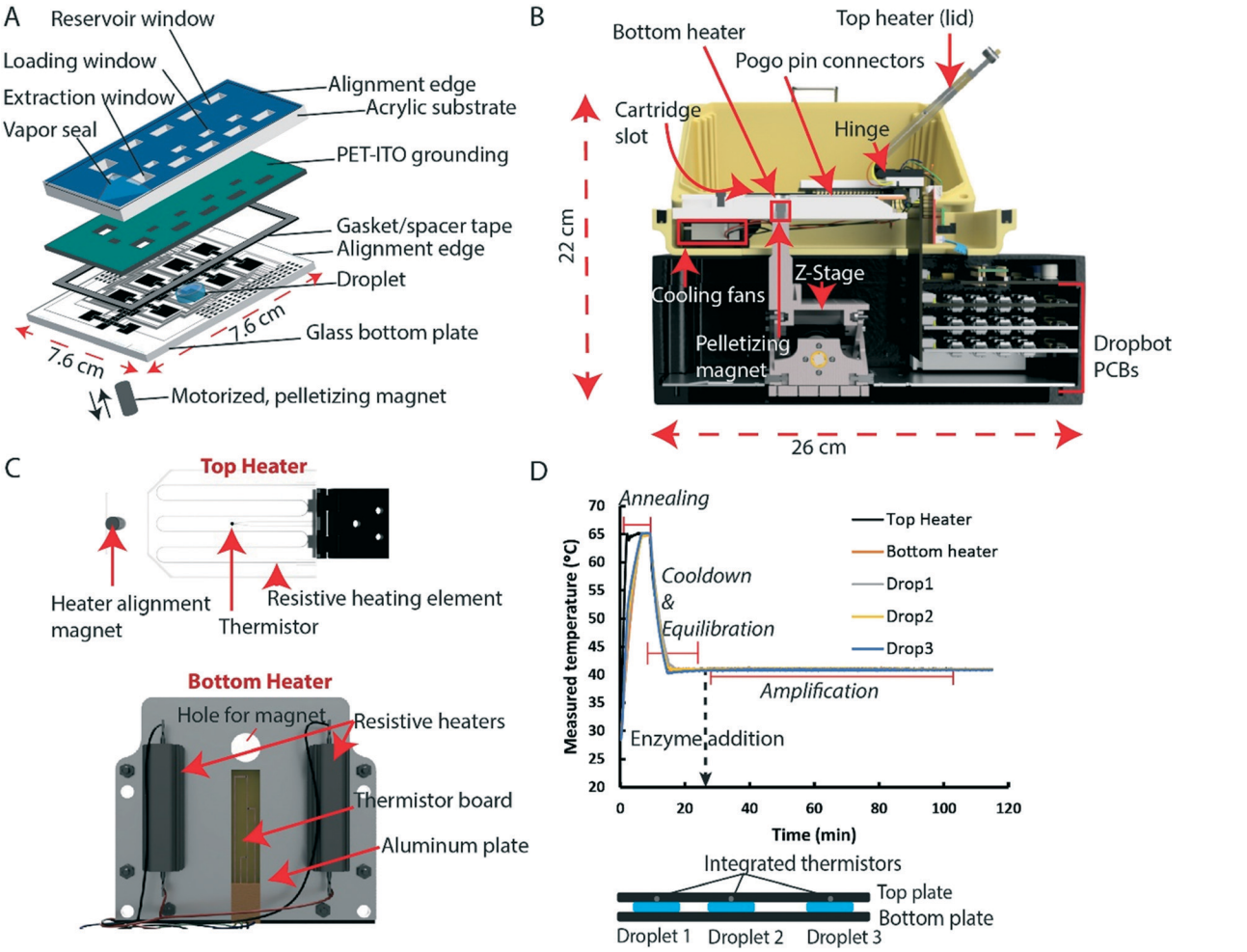

Fig. 2 Zed Box hardware development and testing. A) Schematic showing an exploded view of the DMF cartridge, which comprises a rigid, acrylic substrate (gray) with laser-cut windows for reagent and sample loading, a peelable vapor seal (blue), a flexible, PET-ITO electrical grounding layer (green), a gasket and gap-height spacer (gray), and a glass bottom plate. A liquid droplet (blue disc) is sandwiched between the bottom plate and the PET-ITO substrate. A motorized, pelletizing magnet is located under the bottom plate within the control hardware. B) Cross-sectional view of the Zed Box control hardware, showing the placement of the two resistive heaters, one of two cooling fans, a pelletizing magnet mounted on a motorized *z*-stage, and control electronics (Dropbot PCBs). The DMF cartridge is loaded into the box, and interfaces with the control electronics *via* pogo-pin connectors. When in use, the top heater is lowered so the cartridge is in conformal contact with both heaters. C) Detailed diagrams of heaters. The top heater (top) consists of a milled acrylic scaffold with an embedded resistive heater and a temperature sensor (thermistor). The top heater is mounted on a hinge and can be raised or lowered over the device. The bottom heater (bottom) consists of a milled aluminum conductor with two heating resistors and a thermistor board. A through-hole allows the pelletizing magnet (shown in panel A) to pass through. D) Plot of temperatures measured for three 5 μL buffer droplets (gray, yellow and blue) as a function of time during a simulated NASBA run. The droplets were heated to 65 °C for 2 minutes, followed by incubation at 41 °C for 90 minutes. Overlaid with the droplet temperature measurements are the measured temperatures from the top (black) and bottom (orange) heaters. Labels indicate the steps (annealing, cooldown & equilibration, enzyme loading and amplification) in a typical NASBA run. (Inset) Cartoon illustrating the position of sample and control droplets (in lanes 1–3 in the cartridge) relative to the thermistors in a custom test-cartridge designed for temperature validation.

force set to 7, 1, and 25 respectively). The cut tape was then transferred to the acrylic part by peeling its lower liner, joining the exposed adhesive with the acrylic, and leaving the upper liner on. Tape-lined acrylic pieces were then assembled with the PET-ITO part, by peeling the upper liner (exposing the adhesive) from the former, joining the two, and then smoothing the combined part using a roller to eliminate bubbles. When assembled, the outer edges of the acrylic and PET-ITO windows were flush, with bendable 2 mm flaps of PET-ITO extending into the acrylic windows on the inner edges. Finally, assembled acrylic/PET-ITO parts were dip-coated with 2% w/w FluoroPel PFC 1101V/PFC110, mounted on a spin-coater and spun at 2000 rpm for 30 s, and then dried at room temperature for 30 min.

After assembly of top plates, DMF cartridges (Fig. 2A) were completed in three steps. First, adhesive gaskets were formed from AR-Care® medical grade tape. Three layers of tape were joined and pressed to create a 180 μm thick, double-sided adhesive sheet, with each adhesive side ("upper" and "lower") protected by a liner. The sheet was laser-cut into hollow rectangular gaskets (outer dimensions: 7.5 cm × 5 cm, inner dimensions: 7 cm × 4.2 cm), and the lower liner was removed and the exposed adhesive was affixed to a bottom plate. Second, a top plate (Fluoropel-coated acrylic/PET-ITO) and bottom plate (Fluoropel/parylene-coated chromium coated glass with gasket) were sprayed with 70% v/v ethanol in water, and then were exposed to a UV-treatment for 20 min in a VWR® PCR Workstation containing two UV light tubes (254 nm, 25 W). Third, the upper liner on the gasket was removed, and the top plate was positioned on the bottom plate (adhering to the gasket) using the edges of the two plates and the edges of the reservoir electrodes as alignment markers. The plates were thus joined, resulting in a cartridge defining a fluidic chamber measuring 7 cm × 4.2 cm × 180 μm ($w \times l \times h$). Upon joining, the gasket was observed to undergo a slight compression, resulting in a 'unit droplet' volume occupied by a single 2.8 × 2.8 mm driving electrode of ~1.25 μL. Finished cartridges were packaged in foil pouches for later use. Finally, custom cartridge seals were formed from PCR plate sealing film (Microseal 'B'™), which was laser-cut (at power, speed, and vector current set to 20%, 100%, and 20% respectively) into 8 cm × 5 cm pieces. A rectangular region in the center of each cartridge seal, positioned to align with the region of the cartridge containing the five loading windows, was scored using a laser cutter such that this portion of the seal could be selectively 'peeled off' for access to these windows when needed. Two custom cartridge seals were formed to accompany each cartridge/experiment.

Control hardware design and assembly

The DMF instrument or "Zed Box" was derived from a predecessor (MR Box v2 (ref. 29 and 30)) with a long list of new features added for the current application. All operations in the Zed Box were managed *via* a custom, in-house built peripheral control board. This device (a PCB designed in KiCad), hosts a microcontroller (ATmega328P, Microchip Technology Inc.), two high-power transistors (SQJA60EP-T1_GE3, Vishay Siliconix) for controlling peripheral heating units, two low-power transistors (DMG2302U-7, Diodes Incorporated) for controlling peripheral cooling fans and LEDs, a stepper driver (A4988, Pololu) for controlling the actuation of the pelletizing magnet, and a temperature/humidity sensor (HIH6030-021-001, Honeywell) for logging the external temperature and relative humidity of the environment. The peripheral control board also contains female pin headers to interface with a "bridge" board. The latter (also a custom PCB designed in KiCad) includes interfaces to six custom boards purchased from Sci-Bots Inc. (Kitchener, ON), adapted from DropBot v.3: a (main) DMF control board, three high voltage switching boards (each of which can manage 40 independent DMF electrodes), a pogo-pin board, and a high voltage booster circuit. Finally, the peripheral control board features custom 12 V and 3 V power outlets that were used to power the onboard electronics and all the external devices, and a USB interface to allow communication with a host computer.

The Zed Box was designed to be controlled by a host computer (a laptop) running the open-source DMF control software Microdrop (**https://microfluidics.utoronto.ca/dropbot/**). A custom plugin for Microdrop was written in Python which permitted the user to program and control all of the DMF operations as well as the states and timings of each of the peripheral devices in the instrument from within the Microdrop user interface. Among the tasks managed by the plugin is communication with the microcontroller *via* a custom C++ firmware package which includes a proportional–integral–derivative (PID) algorithm to allow fine control of two heating units on the basis of temperature readings from thermistors as feedback (see below).

When used in DMF operations, a completed DMF cartridge was connected to a custom manifold that permitted Zed-Box-controlled pogo-pins to interface with the chromium contact traces on the bottom plate of the cartridge. Droplets were actuated by applying 100 V_{RMS} square waves at 10 kHz (parameters determined to generate forces below velocity-saturation[41] for the liquids used here) in pre-programmed steps to facilitate droplet dispensing, moving, and mixing. A custom GUI (operating in MicroDrop) was written to guide the user step-by-step through the extraction and amplification process described here, including prompts for all sample and reagent loading and collection steps. In each loading step, the user pipettes a reagent into the appropriate window while the relevant electrode (under the window) is actuated, pulling the fluid under the relevant 'flap' (see details above). All solutions other than lysis and wash buffers (including pre-processed samples and controls) were supplemented with 0.05% (v/v) Tetronic 90R4 to facilitate droplet movement.

Temperature control

As indicated above, the Zed Box included two independent resistive heating units (bottom and top heaters) and a pair of cooling fans (4010, WINSINN, Amazon.ca). The bottom

heating unit consisted of an aluminum plate with two chassis mount resistors (10 Ω, THS5010RJ, TE Connectivity) positioned 33 mm on either side of center of an aluminum plate (108 mm × 95 mm × 1.65 mm, $w \times l \times h$, McMaster-Carr). A custom 11 mm × 65 mm thermistor manifold was mounted in the center of one side of the plate. Briefly, the manifold was formed from copper-coated Kapton® film, with traces patterned into a circuit that interfaced with three soldered negative temperature coefficient (NTC) thermistors (10 kΩ, NTCG103JX103DTDS, TDK Corporation). The top heating unit comprised a 45 cm resistive heating wire (11 Ω, 32-gauge Clapton coil, GiniHomer LifeMods) and an NTC thermistor (10 kΩ, MC65F103A, Amphenol Advanced Sensors) sandwiched between two sheets of PMMA (48 mm × 95 mm × 3 mm, $w \times l \times h$, McMaster-Carr). Thermistor signals were fed into the peripheral control board as feedback for the PID algorithm for error e (the difference between set-point value and measured value) as a function of time t, indicated below,

$$\mathrm{CO}(t) = K_\mathrm{p} e(t) + K_\mathrm{i} \int_0^t e(\tau)\mathrm{d}\tau + K_\mathrm{d} \frac{\mathrm{d}e(t)}{\mathrm{d}t}$$

where the proportional term (K_p), integral term (K_i) and derivative term (K_d) of the PID controller were tuned to 100 °C and 70 °C for the bottom and top heating units, respectively, to determine the computed output (CO). Depending on user input, the PID controller was used to drive temperature changes *via* pulse width modulation (PWM) applied to the heaters. Any increase in temperature to 5 °C above the set temperature triggered the cooling fans for faster cooldown. To evaluate the performance of the heating system, a custom test-cartridge was formed to integrate three thermistors directly above each of three droplets placed in the device. The laser-cut acrylic substrate of the top plate in this cartridge was modified *via* milling to include a gap for a copper coated Kapton® film manifold interfaced with three thermistors between the acrylic and the PET-ITO sheet. The ability of the DMF heating system to set and hold temperatures at 65 °C and 41 °C for integrated sample/control amplification steps (described below) was verified using the custom test cartridge.

In preliminary experiments, the temperature control system (with regular top plates) was used to evaluate droplet-evaporation mitigation strategies, including (i) devices enclosed with adhesive gaskets, (ii) devices enclosed with adhesive gaskets in which droplets were suspended in an oil-shell, and (iii) devices enclosed with adhesive gaskets and PCR-film seals. Briefly, to test conditions (i) and (iii), three 5 μL droplets of PBS (with 0.1% w/v Tetronics 90R4) were dispensed onto an array in an appropriately prepared cartridge. In (ii), a similar procedure was followed, but each droplet was encased in a 1 μL immiscible 'shell' of PCR encapsulation oil (Vapor-Lock®, Qiagen). An image of each droplet was collected using an external camera. The temperature was set to 45 °C and droplets were held stationary for 20 min, after which each droplet was imaged again. A simple image processing algorithm was implemented to identify droplet boundaries and to extract the apparent area occupied by each droplet (in pixels), and ratios of areas before and after heating were used to assess evaporation rate.

Finally, an external tube heater was developed for use as an ancillary system to the DMF platform, for thermal lysis of virus particles. Briefly, a part was designed to hold a single 600 μL Eppendorf centrifuge tube in Fusion360 and 3D printed in High Temp Resin using the stereolithographic 3D printer Form 2 (Formlabs). A 20 cm resistive heating wire (5 Ω, 32-gauge Clapton coil, GiniHomer LifeMods) was looped around the 3D printed part, and an NTC thermistor (10 kΩ, MC65F103A, Amphenol Advanced Sensors) was inserted at the bottom of the part to provide temperature feedback. The tube heater module was controlled by the Zed Box and the computer along with the other peripheral units.

Synthesis of molecular reagents and viral samples

Molecular reagents. The terms 'switch DNA' and 'trigger DNA' correspond to the DNA template for the RNA toehold switch-based sensor and the DNA template for the RNA sequence that triggers switch transcription, respectively. Primary switch and trigger DNA (with sequences reported elsewhere[38]) were synthesized and transfected into DH5-α competent *E. coli* using previously published methods.[37,38] Briefly, switch and trigger pET DNA plasmids were purified from separate overnight cultures using a Qiagen Miniprep™ kit (Hilden, Germany). The two plasmids were linearized *via* polymerase chain reaction (PCR) with Q5® High-Fidelity DNA Polymerase (New England Biolabs, Ipswich, MA), and the linearized DNA products were then purified with Qiagen RNeasy® kit. For experiments with an RNA trigger, the linearized DNA trigger was used as the template for a HiScribe™ T7 high yield RNA synthesis kit (New England Biolabs). Absorbance ratios of DNA (260 : 280 nm) and RNA products (230 : 260 : 280 nm) were determined with a Nanodrop One (Thermo Fisher Scientific; Waltham, MA) and concentrations were subsequently calculated with Beer's law.

Lentivirus synthesis. Lentivirus samples bearing the short target segment of the Zika RNA genome were synthesized using previously a published method.[33,35] Briefly, HEK293T cells were cultured in Dulbecco's modified Eagle medium (DMEM) supplemented with 10% FBS and 1% penicillin–streptomycin at 37 °C at 5% CO_2 in 10 cm plates. Cells were grown to 70% confluency and then transfected with a third-generation lentiviral vector system (pUltat-hot) containing the target Zika viral RNA fragment and the gene mCherry. Following a medium change at 12 h after transfection, cells were cultured until mCherry expression was detected. The viral supernatant was then collected and concentrated using Lenti-X Concentrator™ (TaKaRA Bio Inc., Shiga, Japan) as described by the manufacturer. The resulting virus was quantified using serial dilution of the lentivirus preparation to determine the tissue culture infectious dose required to

infect 50% of the cell monolayer ($TCID_{50}$). The $TCID_{50}$ was then converted to plaque forming units (PFU) using the ATCC calculation.[42] The quantified virus suspension ($\sim 10^7$ PFU mL^{-1}) was stored at −80 °C until use.

Zika virus culture. Zika virus strain PE243 (GenBank access code: KX197192.1) originally isolated from the serum of a Brazilian patient infected with Zika in 2015, was cultured at Oswaldo Cruz Foundation (FIOCRUZ), Pernambuco, Brazil. Briefly, the virus was propagated in Vero cells using Dulbecco's modified medium (DMEM, Gibco, Carlsbad, CA) supplemented with 10% inactivated fetal bovine serum (FBS) (Gibco), 2 mM L-glutamine (Gibco), and 100 U mL^{-1} penicillin/streptomycin (Gibco) at 37 °C in 5% CO_2. Subsequently, the virus was titrated in Vero cells by the standard plaque assay method, resulting in a density of 8.0×10^7 PFU mL^{-1}. The equivalence between PFU and RT-qPCR cycle threshold was determined using methods described elsewhere.[43] After titration, the Zika virus was stored at −80 °C for downstream applications.

Samples, EA controls, and process flow

Samples comprised (i) trigger RNA, (ii) modified lentivirus particles containing trigger RNA or (iii) cultured Zika virus, spiked in matrix (either nuclease-free water or healthy human sera). Negative extraction–amplification (EA) controls were matrix only, and positive EA controls were identical to samples, at final concentrations/densities of (i) 10^3 copies μL^{-1} (trigger RNA), (ii) 10^3 to 10^6 PFU mL^{-1} (lentivirus particles), or (iii) 10^4 PFU mL^{-1} (Zika virus particles). In each analysis of one or more samples, at least one pair of EA positive and controls was analyzed in parallel. All samples and EA controls were subjected to a four-step regimen of pre-processing (P), extraction (E), amplification (A), and cell-free protein expression assay (C). Variations of these steps applied to different types of samples and controls are described below, identified with subscripts 'man' for manual and 'DMF' for DMF operations. For example, a sample processed by DMF was subjected to P–E_{DMF}–A_{DMF}–C, while a positive EA control processed manually was subjected to P–E_{man}–A_{man}–C.

Pre-processing (P)

Samples and EA controls not containing virus were pre-processed using sample lysis reagents from the Genesig Easy® RNA extraction kits, following modified versions of the manufacturer's instructions in five steps. (1) 5 μL of sample or control was mixed with 5 μL lysis buffer containing nuclease-inhibiting guanidine salts. (2) 0.5 μL proteinase K solution was added to the mixture. (3) 1.25 μL carrier RNA solution was added to the mixture. (4) The mixture was incubated at room temperature for 15 min. (5) 12.5 μL of a suspension of RNA-binding magnetic beads was added to the mixture, actively mixed, and incubated at room temperature for an additional 5 min. Samples and EA controls containing virus were treated as above, but with an extra step after the addition of lysis buffer: (1B) the mixture was heated at 95 °C for 2 min in the ancillary tube-heater controlled *via* DropBot, inside a biosafety cabinet per the SOPs laid out by the host institution.

Manual extraction (E_{man})

After pre-processing (P), samples that were processed manually and all EA controls (even those that were amplified by DMF in a later step) were extracted in five steps using extraction reagents from the Genesig Easy® RNA extraction kit. (1) The magnetic beads were pelleted using a magnetic tube rack. (2–4) The supernatant was discarded and the bead pellet was washed twice with 12.5 μL wash buffer and once with 12.5 μL 80% v/v ethanol/wash buffer. (5) The washed bead pellet was air-dried and RNA was eluted into 5 μL of nuclease-free water containing 0.4 U mL^{-1} RNAse inhibitors. In some (characterization) experiments, the extracted RNA concentration was measured using a Qubit® fluorometer following the procedure in the Qubit® RNA BR assay kit, ThermoFisher Scientific.

DMF extraction (E_{DMF})

After pre-processing (P) (using the lysis components of the Genesig Easy® kit), samples were extracted by DMF one-at-a-time in nine steps (using the extraction components of the Genesig Easy® kit). (1) The entire pre-processed sample volume (~24 μL) was loaded and pre-concentrated in the extraction lane (Fig. S1†) using the P-CLIP technique,[44] wherein the pelletizing magnet was engaged, and a continuous pathway of electrodes was activated leading from the sample reservoir to an absorbent waste pad formed from a Wypall® paper towel wick (7 mm × 5 mm) in the waste reservoir [this condition represents the optimum of several that were tested]. The optimum condition was characterized in two tests. (i) The times required to wick 50 μL increments of sample plus preprocessing reagents into the absorbent pad up to a maximum absorbed volume of 250 μL were measured and reported as flow rates. (ii) Standard volumes of pre-processed sample were treated as indicated, and the numbers of beads before and after extraction were measured using a Vi-Cell XR® cell viability analyzer. (2) The bead pellet carrying bound sample RNA was suspended in a 6.25 μL wash buffer droplet (with magnet disengaged) and transported to the clean-up lane in the cartridge (Fig. S1†). (3–8) The sample was run through six successive wash steps, beginning with four washes in five-unit-volume droplets (~6.25 μL each) of wash buffer followed by two washes in five-unit-volume droplets of 80% v/v ethanol/wash buffer. Each of the six wash steps was carried out by dispensing a five-unit-volume droplet of the desired buffer from a reservoir into the clean-up lane, transporting it to the bead pellet, disengaging the magnet to resuspend the bead pellet (with active mixing by manipulating the droplet in a circular pattern for 1 min), engaging the magnet to re-pellet the particles, and driving the (now spent) droplet to waste [in some preliminary experiments, three washes were used

instead of six]. (9) Sample was eluted from the beads into a four-unit-volume droplet (~5 μL) of DI water containing 0.4 U μL^{-1} RNase inhibitors, using a similar sequence of movements described above, with mixing extended to 3 min, and no pelleting or driving to waste. A unit droplet (~1.25 μL) was then split off for amplification.

Manual amplification (A_{man})

After extraction (E_{man} or E_{DMF}), samples and EA controls that were isothermally amplified manually were treated using nucleic acid sequence based amplification (NASBA liquid kit, Life Sciences Advanced Technologies), in a standard benchtop thermocycler (Bio-Rad™) in a three step procedure (volumes indicated here are per sample): (1) 1.25 μL of eluted RNA was added to 2.75 μL of NASBA master mix, which contained kit buffer (1.67 μL), a solution of rNTPs (0.83 μL), solutions of forward and reverse primers (25 μM, 0.1 μL each), and a solution of RNase inhibitors (0.05 μL, for a final concentration of 0.4 U μL^{-1} in the master mix). (2) The combined solution was annealed at 65 °C for 2 minutes, followed by incubating at 41 °C for 10 minutes. (3) 1.25 μL of a solution of NASBA enzymes was then added to the annealed mixture and incubated at 41 °C for 60 to 90 min.

DMF amplification (A_{DMF})

After extraction (E_{man} or E_{DMF}), the DMF isothermal amplification procedure was applied to one sample and a pair (positive/negative) of EA controls in parallel in five steps. (1) Three 2.75 μL aliquots of NASBA master-mix (see A_{man} for make-up of this solution) were separately pipetted into loading windows and driven into the three amplification lanes (Fig. S1†). (2) One 1.25 μL aliquot each of extracted positive and negative EA controls (after E_{man} above) was loaded into its designated amplification lane. Separately, the unit droplet of extracted sample (after E_{DMF} above) was driven into its lane. (3) Each sample or control droplet was then merged and mixed with the NASBA master-mix droplet in their lanes, which were kept three-electrodes-apart at all times, and were located in a dedicated region of the cartridge separate from the extraction and clean up lanes. A custom cartridge seal was manually applied to seal the windows. The box was closed, and an automated annealing regimen was initiated, comprising heating to 65 °C for 2 min for primer annealing, followed by cooling and equilibration at 41 °C for 10 min. (4) The pre-scored seal over the loading windows was manually removed, to allow pipetting of one 1.25 μL aliquot of NASBA enzyme mix (see A_{man} for make-up of this solution) into the loading windows of each of the three lanes. A second cartridge seal was manually applied, the box was closed again, and an automated amplification regimen was initiated, comprising incubation at 41 °C for 1.5 h with continuous, automated mixing. (5) The pre-scored seal over the loading windows was manually removed, and a pipette was used to extract each droplet (sample, positive EA control, negative EA control) into a separate nuclease-free tube.

Cell-free protein expression assay (C)

After amplification (A_{man} or A_{DMF}), samples and controls were evaluated using the toehold switch-based sensor for the Zika virus and the PURExpress *in vitro* protein synthesis kit as described previously.[38] Each analysis tested at least five solutions, including three that were pre-processed (P), extracted (E), and amplified (A) as described above: (i) sample, (ii) positive EA control, and (iii) negative EA control. Two additional controls were also evaluated at this stage – (iv) a cell-free (CF) negative control of RNAse-free water, and (v) a CF positive control comprising the Zika DNA template encoding the RNA trigger, or unamplified RNA at a concentration high enough to elicit a positive reaction (conc. indicated below). Five tubes were prepared as follows: 5.84 μL of cell-free expression assay master mix ['CF master mix', containing enzymes and 5 mg mL^{-1} chlorophenol red-β-D-galactoside (CPRG), in nuclease-free water] were pipetted into each tube, followed by the DNA template encoding the toehold switch to a final concentration of 33 nM in each tube. After this, 1.14 μL of solutions (i)–(iii) were added to the first three tubes. To the fifth tube the appropriate volume of trigger DNA or RNA solution was added to bring the final trigger concentration to 5 ng mL^{-1} (DNA) or 2 μM (RNA). All five tubes were then made up to 8 μL using nuclease free DI water. Occasionally, an additional control was run: (vi) a "no switch negative control", which was identical to the CF-negative control (iv) but without the DNA switch.

Prior to analysis, well-plates were prepared as follows: cellulose filter paper (Whatman #42) was blocked with 5% w/v BSA/water and then cut into 2 mm circles with a biopsy punch. Each punch was positioned at the bottom of a well in a 384-well plate (Corning®, low binding, flat bottom, black), creating a uniform, partially transparent surface. After preparing the five tubes (above), three 2 μL aliquots of each cell free reaction solution were pipetted into individual wells in the pre-prepared well plate, and colour development was monitored at 37 °C for 175 min. In experiments with non-Zika virus samples in Toronto, colour development was quantified *via* optical density measurements collected every 5 minutes (for 175 min) at 575 nm in a Pherastar™ plate reader (BMG Labtech) held at 37 °C, with results visualized using the accompanying Mars™ data analysis software. In these experiments, the plate reader was set to "Absorbance-Plate Mode", with a focal height setting of 10.5 mm, and 10 flashes per well scan per cycle. No path length correction or gain settings were used. In experiments with live Zika virus conducted at FIOCRUZ (Pernambuco, Brazil), paper-lined well plates were instead monitored using an inexpensive, portable well plate imager known as the PLUM, which is described in detail elsewhere.[39] PLUM readings were also collected every 5 minutes for 175 min at 37 °C, as a ratio of blue to green pixels.

CF-negative and CF-positive controls (iv–v) were used for quality checks (QC) to determine whether the reaction proceeded as desired. For those that passed QC, for samples

analyzed using the plate reader, the optical densities (O.D. s) from solutions (i)–(iii) were analyzed using Microsoft Excel™ and plots were generated on GraphPad Prism™ 9. Each solution was analyzed at least twice using separate cartridges, and each replicate was read *via* cell-free reactions split into three wells, giving at least six data-sets per sample or control. For each data-set evaluated by the Pherastar, the average O.D. measured at the endpoint (t = 175 min) from the extracted sample was normalized to average endpoint measurements of the positive and negative controls amplified in the same cartridge per the following formula: (sample $OD_{575\ nm}$ − EA negative control $OD_{575\ nm}$)/(EA positive control $OD_{575\ nm}$ − EA negative control $OD_{575\ nm}$). A similar procedure was followed for image analysis data generated by the PLUM.

Results and discussion

DMF cartridge and hardware development

A digital microfluidic (DMF) system was developed to automate key steps in sample processing for a cutting-edge cell-free Zika virus diagnostic (Fig. 1) as a step toward reducing complexity for operation by inexpert users at the point of care. An exploded view of the DMF cartridge developed to support this workflow is shown in Fig. 2A, and a more detailed view is shown in Fig. S1.† A key novelty of the system reported here is an integrated, automated heating regimen for RNA-primer annealing and amplification. In such systems, substantial fluid (in sample and reagent droplets) can be lost to evaporation.[31] Some common techniques employed to guard against evaporation in DMF include using an immiscible oil-based filler fluid in which aqueous droplets are suspended,[32] using an air filler (like the results presented here) but with aqueous droplets protected by oil film 'shells',[35] or repeated solvent injection of heated solvents to compensate for lost fluid.[36] Though highly effective in the laboratory, these techniques can be difficult to translate to the field as they may require extra user steps (involving filling the device with the oil phase) and additional hardware design and programming (for fluid injection). In addition, systems in which droplets are suspended in oil can be sensitive to device and system orientation (with unwanted droplet drifting and merging[45]); in contrast, those in which droplets are suspended in air are more stable, and can even be operated vertically if needed.[46]

To accommodate the challenge of integrating heating and amplification with droplet-in-air operation, we developed a new approach relying on a custom sealed and humidified cartridge format. The unique top-plate assembly (Fig. 2A) was designed to feature a series of open windows for reagent loading and recovery (featuring flexible, 2 mm, overhanging "flaps" to facilitate uptake of the liquid by the electrode). In addition, the top and bottom plates were assembled using a vapour-proof gasket (that also set the inter-plate spacing for droplet operation). Finally, a custom cartridge seal (with scored regions for selective access) was designed for the long-duration heating steps. To evaluate this strategy, droplet retention at an elevated temperature was quantified and compared experimentally with the oil-shell technique. As shown in Fig. S2,† the oil-free gasket + cartridge seal approach described here limited the evaporation rate substantially, such that droplets retained 93 ± 7% (ave. ± st. dev. for n = 3 droplets) of their initial volumes after incubation at 45 °C for 20 min. The oil-free gasket + cartridge seal strategy was therefore used in all further experiments.

A customized control system known as the "Zed Box" was designed and built to automate the unique DMF workflow required for the application described here. The system is shown in Fig. 1A (enclosed view) and Fig. 2B (cross-sectional view). The outer dimensions were 26 × 19 × 22 cm (l × w × h), and the box weighed ~3.75 kg. A hardware "kit" composed of the Zed Box, a pack of 30 disposable cartridges, a laptop computer and a battery pack can be transported together in a backpack, or as aircraft cabin baggage. The major components of the box (Fig. 2B) included the control electronics, the pelletizing magnet mounted on a motorized Z-stage that moved up or down for magnet engagement and disengagement respectively, and a new thermal module (described here for the first time) consisting of two resistive heaters (Fig. 2C, top and bottom units) and two cooling fans flanking the heaters. While the bottom heater cycled the droplets through the desired temperature steps, the top heater served to reduce condensation on the inside-upper surface of the cartridge, thereby minimizing temperature gradients. This feature was inspired by commercial bench-top thermal cyclers, and proved critical to preventing cross-contamination.

The new thermal module in the Zed Box was designed to facilitate in-line amplification by nucleic acid sequence based amplification[40] (NASBA). In initial prototyping experiments, a number of key control features were determined to be important for successful operation. First, to improve cooling transience, resistors on the bottom heater (Fig. 2C, bottom) were embedded into an aluminum plate. These resistors were chosen as they featured grooves that acted as an efficient heat sink owing to their high surface area. To improve cooling rates, fans were integrated in the system to direct cool air from the environment to the heaters. Second, both heaters were equipped with temperature sensors (thermistors) (Fig. 2C) – three on the bottom heater, designed to reside directly below the amplification lanes on the cartridges, and one on the top heater, which enabled closed loop control *via* a custom proportional–integral–differential (PID) feedback algorithm. The heaters were driven by pulse width modulation (PWM) for fine control of the applied current, and when in operation, all thermistor readings as well as the temperature and relative humidity of the environment were continuously monitored and logged. Overall, the new module allowed for rapid and accurate cycling from 5 °C above room temperature (R.T. + 5 °C) to 80 °C – a range suitable for most isothermal nucleic acid amplification techniques.[47]

Representative thermal transience curves for the new system are shown in Fig. 2D, acquired using a custom test-cartridge designed to feature three thermistors positioned directly above each droplet position in the device (Fig. 2D, inset). These data illustrate the ~114 min temperature cycling protocol for NASBA, which includes ~7 min to heat from R.T. to 65 °C, 2 min for annealing at 65 °C, ~15 min for cooling and equilibration at 41 °C, and 90 min for amplification at 41 °C. A custom MicroDrop plugin managed these heating steps automatically, as well as all droplet movement and pelletizing magnet engagements. The results indicate that the thermistor readings corresponding to the three droplets (Fig. 2D, inset) were in close agreement with the set temperatures of the heaters throughout the process.

Importantly, the resistive heaters used in the Zed Box to achieve the performance indicated above were selected because they have much lower power requirements than thermoelectric heaters. The power consumed by the Zed Box breaks down as follows: (i) the two heaters draw ~4800 mA for the first 3 minutes of operation, after which they are on for ~10% of the duty cycle, (ii) the fans draw ~200 mA when operational, and (iii) the DMF control hardware draws 200–300 mA when operating at full capacity with all channels active. In all, the complete workflow (described below) is run on 12 V DC (made possible by the built-in high-voltage amplifier), which can be supplied by a rechargeable battery pack rated at 10 166 mAh, identical to the one used for a similar instrument in prior work.[29,30] This type of battery back is portable (weighing only 0.5 kg), and two such packs are sufficient to power the Zed Box for a full day of work. Of course, the use time is unlimited when powered by electrical mains.

Cell-free protein expression assay and detector

The cartridges and Zed Box described here were designed to process samples upstream of analysis by a state-of-the-art, cell-free, toehold switch-based assay for the detection of Zika virus RNA.[37] The working principle of the assay is described in the introduction and is shown in Fig. S3,† where the key component is the toehold switch – a riboregulator comprising a synthetic RNA sequence complementary to the analyte (specific to a portion of the Zika genome known as the 'trigger RNA') – upstream of a *lacZ* reporter sequence. In the absence of a target sequence, reporter gene expression is repressed because of the RNA switch's hairpin loop structure, which prevents ribosome binding. In the presence of analyte (the target sequence), the switch linearizes, freeing the ribosome binding site (RBS) upstream of the *lacZ* gene, which (in the presence of cell-free expression enzymes) causes the translation of β-galactosidase. In turn, this results in conversion of the yellow substrate (chlorophenol red β-D-galactopyranoside, or CPRG) to a deep red product (chlorophenol red, or CPR) at a rate that corresponds to the rate of β-galactosidase expression. This colour change is quantified *via* optical density measurements at 575 nm, and in experiments was validated by a set of controls for the cell-free expression assay (CF positive/negative controls) and for the extraction and amplification procedure (EA positive/negative controls).

As shown in Fig. S4,† data were typically collected every five minutes during a 175-minute period (for diagnostic purposes). For quantitation, the endpoint OD 575 nm measured at t = 175 min after the start of the assay was normalized and recorded as the signal for that sample. In the work described here, absorbance measurements were collected off-chip, in a commercial plate reader (for laboratory experiments) or the portable PLUM reader[39] (for field work). In the future, the absorbance detection for the cell-free expression assay might be implemented using a related portable DMF system with camera/automated-filter-changer system.[48] Alternatively, the cell-free expression assay might (in the future) be replaced by assessing product formation during the amplification stage using molecular beacon probes[49] in a portable DMF system designed for fluorescence detection.[48]

Optimization of DMF extraction and amplification

The primary goal for this work was to develop an automated microfluidic system for analyte extraction from matrix (in this case, plasma) and target amplification (in this case, by NASBA), steps that are often overlooked in microfluidic diagnostic systems. We developed manual and DMF variations of procedures for extraction (E_{man} & E_{DMF}) and amplification (A_{man} & A_{DMF}), which were paired with off-chip pre-processing (P) and cell-free protein expression analysis (C) procedures. Substantial optimization of these steps was required, which is reviewed here.

The sample extraction protocol was adapted from Genesig Easy® extraction kits, in which samples are lysed, mixed with reagents, and then subjected to magnetic bead pulldown. Four key optimization steps were enacted. (1) The kit, which is designed for extraction of high-concentration samples, was optimized for low-concentration RNA capture. Most of the manufacturer's suggested ratios of reagents to sample were found to be acceptable for this application, with the exception of the RNA carrier solution, a reagent that promotes electrostatic binding of sample RNA to magnetic beads. In preliminary experiments with synthetic Zika RNA standards processed by P–E_{man}–A_{man}–C, it was found that increasing the amount of RNA carrier by 10-fold relative to the manufacturer's instructions resulted in reproducible detection of analyte signal at concentrations as low as 1 copy per μL (Fig. S5†), so this approach was used for all analyses reported here. (2) The kit, which is designed for extraction of high-volume samples (>200 μL), was optimized for low volumes. Several scaled-down reagent formulations (Table S1†) were tested and applied to Zika RNA standards (P–E_{man}–A_{man}) with results probed by fluorimetry. As shown in Fig. S6,† the extraction efficiency for all conditions was approximately 80%; thus, the smallest scale tested (with 5 μL sample) was used here. (3) Even after scaling down the

volumes, the final sample/bead-suspension in the pre-processed mixture is >24 μL, a volume that is too large for the standard DMF devices used here. Thus, the DMF pre-concentration by liquid intake by paper[44] (P-CLIP) technique was adapted to extract analytes into a smaller volume for further processing on-chip. Briefly, in P-CLIP, a magnet is engaged while a large-volume sample is driven across a DMF device, propelled by wicking into an absorbent pad (Fig. S7, steps i–iii†). Then, after wash steps, RNA on the beads is eluted in a small droplet, where it is ready for further treatment (Fig. S7, steps iv–vi†). The P-CLIP procedure used here was optimized for relatively constant flow rate of ~0.35 μL s^{-1} during bead-loading (Fig. S8†), and under these conditions, bead-counts revealed 97 ± 4.8% (ave. ± std. dev. for n = 3 replicates) bead recovery, which was deemed adequate for this application. (4) According to the kit, magnetic particles are to be washed by resuspending and pulling down twice in aqueous buffer and a third time in 80% ethanol. When the same three-wash procedure was applied on DMF to Zika RNA standard (evaluated as P–E_{DMF}–A_{DMF}–C), reduced signals were observed in the resulting toehold switch assays (Fig. 3A). As shown, this deficit was reversed by doubling the number of washes in the DMF procedure (four aqueous, two 80% ethanol) which was adopted as the standard process. After optimization of all parts of the process (1–4 above), the DMF extraction procedure was stable, reproducible, and completely automated, requiring 30 minutes from sample loading to elution, such that samples were ready for amplification.

The amplification protocol selected for this work was NASBA, which has been used previously in enclosed droplet-in-channel devices,[19,20] but as far as we are aware this is the first report of its use in the open 'DMF' format. We propose that NASBA is particularly well suited for DMF, as in contrast to several isothermal alternative schemes, NASBA does not require the use of crowding agents like PEG that can increase viscosity/reduce velocity in DMF devices. For example, in initial tests evaluating NASBA reagents and reverse transcription-recombinase polymerase amplification[50] (RT-RPA) reagents (which contain PEG/crowding additives), the NASBA formulations were found to be more reliable for high-velocity droplet movement than the alternative. Other factors favouring the selection of NASBA for this application included its production of amplified RNA (instead of DNA) such that switch expression can be triggered directly,[38] as well as its high sensitivity.[51,52]

The NASBA protocol used here was adapted from Life Sciences Advanced Technologies kits, in which samples are mixed with nucleotides, primers, and RNase inhibitors and annealed at 65 °C, and then cooled and mixed with enzymes to react at 41 °C. Two key optimizations were enacted to allow for seamless automation of this procedure by DMF. (1) The NASBA reagent mixtures were supplemented with 0.1% (v/v) Tetronics 90R4, an additive that has previously been reported to be useful[28] for enabling the manipulation of 'sticky' solutions that are not otherwise movable by DMF. This modification was found to be particularly important for reproducible dispensing and metering of NASBA reagents during amplification (required for full automation). (2) The duration of the 41 °C reaction-step was also extended to 90 min (relative to the 60 min duration recommended by the manufacturer), to allow for reproducible detection of samples

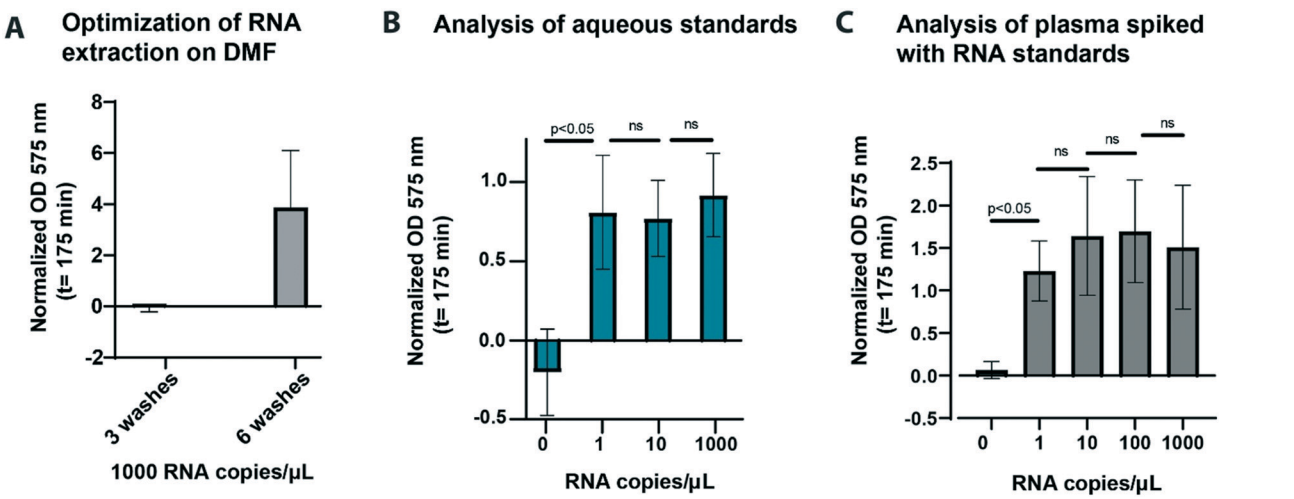

Fig. 3 Optimization of DMF extraction and amplification procedures. A) Plot of normalized, end-point (t = 175 min) OD 575 nm readouts for the cell free expression assay after DMF extraction with three (black) or six (gray) bead-wash-steps and DMF amplification of plasma containing Zika trigger RNA at 1000 copies per μL. Error bars represent 1 std. dev. from n = 5 replicates in each condition. B) Plot of normalized, end-point (t = 175 min) OD 575 nm readouts for the cell free expression assay after amplification on-chip of serially diluted Zika RNA standards in water. Error bars represent ± 1 std. dev. from n = 3 replicates in each condition; t-test comparisons indicate $p < 0.05$ or non-significant (ns). C) Plot of normalized, end-point (t = 175 min) OD 575 nm readouts for the cell free expression assay after extraction and amplification on-chip of Zika RNA spiked in healthy human plasma. Error bars represent ± 1 std. dev. from n = 3 replicates in each condition; t-test comparisons indicate $p < 0.05$ or non-significant (ns).

containing 1 copy per μL of analyte. A five-step DMF procedure was developed to automate the amplification protocol, with temperature programming performed automatically in the Zed Box (Fig. 2D). To minimize cross-contamination driven by satellite droplet ejection[53] or aerosol cross-talk, droplets containing the amplification reaction were kept three-electrodes-apart throughout the procedure. The process lasted 2 hours (for amplification only), or 2.5 hours including extraction. The net effect of all of the optimizations described above was a robust method capable of reproducible detection of samples containing physiological Zika RNA copy numbers in infected patients.[54] For example, aqueous standards of Zika trigger RNA concentrations of 1, 10 and 1000 copies per μL in water (n = 3) were processed end-to-end on DMF (P–E_{DMF}–A_{DMF}–C) and tested significantly higher than comparable samples lacking analyte (n = 3) (Fig. 3B). More importantly, spiked standards in human plasma also tested significantly higher than Zika RNA-free plasma samples (n = 3) (Fig. 3C).

In sum, the new protocol allowed for end-to-end automation of steps that are often neglected in microfluidic molecular diagnostic assays – extraction and amplification. As with any new technique, there is room for improving the process in the future. For example, in the current protocol, the Zed Box prompts the user at various stages to load reagents for extraction and amplification; in the future, these steps might be "hidden" from the user by incorporating dried/stored reagents on the cartridge to be rehydrated on-demand.[55] Likewise, device geometry constraints limited the current method to evaluating one sample at a time, with EA controls extracted manually prior to loading onto the cartridge for amplification in parallel with the sample. In the future, new technologies featuring DMF devices relying on large electrode arrays[56,57] might allow for multiple samples and all controls to be run in parallel, end-to-end. Finally, as indicated above, in the future, detection might be incorporated into the Zed Box for a process that is completely hands-free.

Finally, we note that there are commercial diagnostic systems that integrate sample extraction and amplification, including the Cepheid GenXpert™[58] and the Revogene® SARS-Cov-2 platform.[59] These and similar products are wonderful – highly engineered, validated, with regulatory approval, *etc.* The home-made system described here is in a much earlier stage of development, but has some advantages, including smaller footprint, battery-pack operation, and an open-source architecture that offers great flexibility for protocol development, potentially allowing a wide range of sample-types and applications to be developed.

Method validation

Armed with an optimized, automated protocol for Zika virus detection (P–E_{DMF}–A_{DMF}–C), attention was turned to validation of the method with blinded samples. As a first validation step, fifteen single-blinded, spiked plasma samples containing Zika trigger RNA were formed at concentrations between 1 and 100 copies per μL (positive) or 0 copy per μL (negative), respectively. Two different operators ran two Zed Boxes in parallel with a throughput of four samples (plus two EA controls per sample) per 8-hour per day. Four of the fifteen runs performed were discarded due to unusual reads on their EA controls. After unblinding, a scatter plot (Fig. 4A) and a receiver operating characteristic (ROC) curve[60,61] (Fig. 4B) were generated in reference to the known values of trigger RNA concentration in the samples. The ROC curve had AUC = 0.86, and a threshold was selected for 100% sensitivity and 75% specificity, following the standard practice for portable diagnostics for infectious disease[62] to prioritize sensitivity (minimizing false negatives) at the expense of specificity (risking false positives). Note that the imperfect selectivity in this small sample set came from a single false positive, which had a normalized signal that was a close match to that of the positive EA control. This suggests the possibility of cross-contamination (which emphasizes the importance of controlling for this phenomenon) or simple mis-labeling. Whatever the explanation for this result, this performance was deemed sufficient for further testing.

As a second validation step, we turned to the evaluation of samples containing virus particles. In preliminary studies in Toronto with a surrogate sample-type (lentivirus encapsulating a short segment of the Zika RNA genome[39]), it was determined that the pre-processing step (P) should be modified to include thermal treatment in addition to the chemical lysis applied to samples not containing viral particles (Fig. S9A†), likely because the heat breaks open viral capsids and inactivates sample nucleases more effectively than treatment with lysis buffer and proteinase-K alone.[63] In these experiments, heat lysis proved especially useful for decreasing the background and reducing variability in the blank samples (0 PFU mL^{-1}), permitting the distinction of positive samples from the blank. This drove the development of a late addition to the Zed Box, an ancillary tube-heater (Fig. S9B†). This unit, which relies on the same PWM and PID control as the top and bottom heaters in the Zed Box chassis (Fig. 2C) is controlled by the Zed-Box hardware and a Jupyter notebook script, which prompts the user to insert the sample into an Eppendorf tube for heating at 95 °C for 2 min, prior to loading into the device to begin the automated extraction and amplification procedures.

Two Zed Box instruments with an ancillary tube-heater were transported to Recife, Brazil for evaluation with samples containing active Zika virus particles. Preliminary studies validated the importance of the thermal lysis step (Fig. S9C†), and the systems were applied to evaluating Zika virus cultures end-to-end on DMF (P–E_{DMF}–A_{DMF}–C). In these final proof-of-concept tests, rather than using an expensive, multi-mode plate reader, the portable PLUM reader[39] was used. As shown in Fig. 4C, samples containing 100 and 10 000 PFU mL^{-1} Zika virus (amounting to 0.5 and 50 PFU per 5 μL sample, with particle densities corresponding to RT-qPCR cycle threshold values of 32.0 and 19.8 respectively per Table S2†) tested significantly higher than blank samples, while

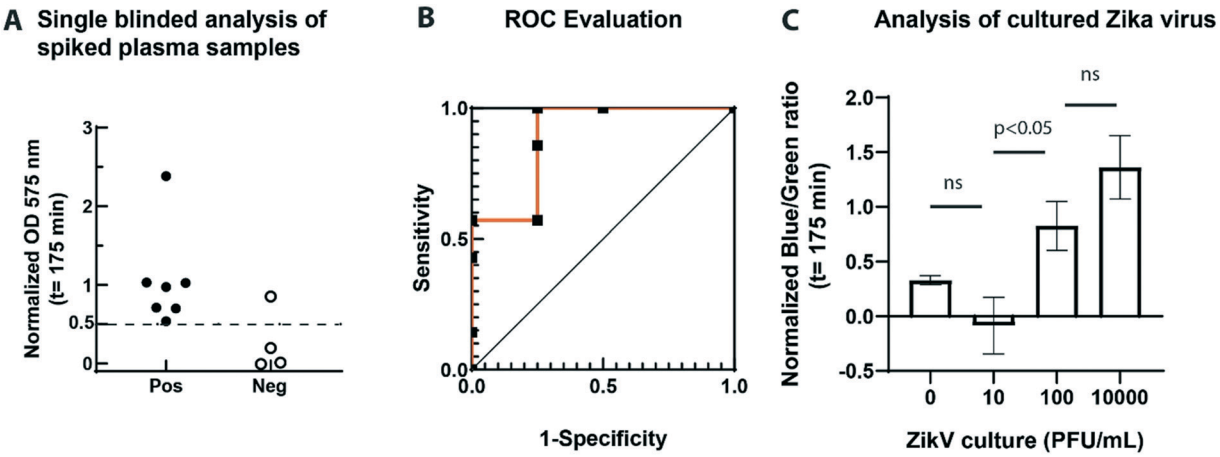

Fig. 4 Validation of the DMF Zika virus analysis method. A) Vertical scatter plot of normalized, end-point (t = 175 min) OD 575 nm readouts for the cell free expression assay after extraction and amplification on-chip tested in a blinded evaluation study performed on artificially spiked human plasma. A threshold (y = 0.5) was drawn based on analysis in (B). B) Receiver operator characteristic (ROC) analysis of the same samples from (A). At the optimal threshold (y = 0.5), the area under the curve (AUC) is 0.86, and sensitivity and specificity are 100% and 75% respectively. C) Plot of normalized blue/green ratios for the cell free expression assay of dilutions of cultured Zika virus/water, performed in Recife, Brazil using the PLUM portable well-plate reader, after thermal lysis and extraction and amplification on-chip. Error bars represent ± 1 std. dev. from n = 3 replicates in each condition.

samples containing 10 PFU mL^{-1} (amounting to 0.05 PFU per sample, cycle threshold value 37.9) were not distinguished from the blank. The latter might be related to RNA degradation during or after processing of these samples, or may indicate that this is beyond the detection limit for this process and configuration.

The results described here are in close agreement with prior work done to verify the toehold switch using Zika virus cultures generated in the same laboratory.[38] Overall, this performance level should be sufficient to detect viral loads in the urine of infected patients[64] and to detect some (but not all) infections in patient plasma or cerebrospinal fluid.[64] While there is some room for improvement (including the potential upgrades described above), the system appears to be suited for portable Zika virus diagnostic assays, a hypothesis that may be tested in the future. Most importantly, we propose that the automated sample extraction and amplification schemes described here are likely to be commutable to many other molecular diagnostic assays in the future. Whatever schemes are used, we encourage the community to consider including integrated and automated sample processing into the next generations of portable molecular diagnostic assays.

Conclusions

We developed a portable, integrated DMF platform to process biological samples prior to downstream molecular diagnostic analysis. The new DMF system was used to extract and selectively amplify Zika RNA from small volumes (5 μL) of simulated aqueous and plasma samples, as well as suspensions of lab-grown Zika virus. This is the first digital microfluidic method that we are aware of for sample processing upstream of a one-pot colorimetric assay for the detection of amplified RNA. Our results indicate a limit of detection for free RNA in plasma is close to 1000 copies per mL, and between 10 and 100 PFU mL^{-1} in samples containing Zika virus particles. The latter were equivalent to RT-qPCR cycle threshold values of 37.9 and 32.0 respectively, which are within physiological levels in infected patient urine (and in some cases, serum). Given its small footprint, light weight, and capacity to run off a 12 V battery pack, we have demonstrated that this system and its accessories can be transported in a backpack or in an aircraft cabin, and in the future might be used remotely for infectious disease outbreak surveillance. Most importantly, the system addresses an overlooked area of laboratory automation and on-site testing – sample processing prior to analysis. The methods described here are relatively general, and should be applicable to other targets and applications in the future.

Author contributions

T. N., J. D., T. K., M. S., and A. R. W. planned experiments. T. N., I. C., J. D., T. K., and M. S. executed experiments. T. N. and I. C. compiled and analyzed the data. J. D. and A. A. S. designed, built and tested the DMF and temperature control hardware and made the necessary modifications to the control software. M. H. designed the DMF top plate and tested the humidity seal. C. D. and J. L. assisted with process optimization, and D. G. R provided preliminary planning and management support. K. P. provided the DNA encoding the Zika trigger, toehold switch, and lentivirus samples, and the PLUM plate reader, along with project support. M. S. synthesized switch and trigger reagents used for this work. S. J. R. d. S. and L. P. generated the Zika virus culture and provided logistic support in Brazil. T. N., J. D., A. A. S., and A. R. W. wrote the manuscript, with contributions from all authors.

Conflicts of interest

There are no conflicts to declare.

Acknowledgements

We acknowledge the support from the CIHR/IDRC Team Grant: Canada-Latin America-Caribbean Zika Virus Program (FRN: 149783) and the University of Toronto's Major Research Project Management Fund (KP). We also thank NSERC for funding this project, and Dr. Margot Karlikow, Livia Guo, and Seray Cicek (all at U of T) for detailed advice and fruitful conversations. A. R. W. thanks the Canada Research Chair (CRC) program.

References

1 C. Chang, K. Ortiz, A. Ansari and M. E. Gershwin, The Zika outbreak of the 21st century, *J. Autoimmun.*, 2016, **68**, 1–13.
2 J. Bedford, *et al.*, COVID-19: towards controlling of a pandemic, *Lancet*, 2020, **395**, 1015–1018.
3 B. Brehm-Stecher, C. Young, L. A. Jaycus and M. L. Tortorello, Sample preparation: the forgotten beginning, *J. Food Prot.*, 2009, **72**, 1774–1789.
4 D. Zhang, *et al.*, A paper-based platform for detection of viral RNA, *Analyst*, 2017, **142**, 815–823.
5 L. Magro, *et al.*, Paper-based RNA detection and multiplexed analysis for Ebola virus diagnostics, *Sci. Rep.*, 2017, **7**, 1347.
6 I. Hongwarittorrn, N. Chaichanawongsaroj and W. Laiwattanapaisal, Semi-quantitative visual detection of loop mediated isothermal amplification (LAMP)-generated DNA by distance-based measurement on a paper device, *Talanta*, 2017, **175**, 135–142.
7 S. Kersting, V. Rausch, F. F. Bier and M. von Nickisch-Rosenegk, Rapid detection of Plasmodium falciparum with isothermal recombinase polymerase amplification and lateral flow analysis, *Malar. J.*, 2014, **13**, 99.
8 K. M. Byers, A. R. Bird, H. D. Cho and J. C. Linnes, Fully Dried Two-Dimensional Paper Network for Enzymatically Enhanced Detection of Nucleic Acid Amplicons, *ACS Omega*, 2020, **5**, 4673–4681.
9 J. Reboud, *et al.*, Paper-based microfluidics for DNA diagnostics of malaria in low resource underserved rural communities, *Proc. Natl. Acad. Sci. U. S. A.*, 2019, **116**, 4834–4842.
10 E. D. Goluch, Microbial Identification Using Electrochemical Detection of Metabolites, *Trends Biotechnol.*, 2017, **35**, 1125–1128.
11 P. Bhandari, T. Narahari and D. Dendukuri, Fab-Chips: A versatile, fabric-based platform for low-cost, rapid and multiplexed diagnostics, *Lab Chip*, 2011, **11**, 2493–2499.
12 H. J. Sismaet, A. J. Pinto and E. D. Goluch, Electrochemical sensors for identifying pyocyanin production in clinical Pseudomonas aeruginosa isolates, *Biosens. Bioelectron.*, 2017, **97**, 65–69.
13 ThermoFisher Scientific, The Basics: RNA Isolation, Available at: **https://www.thermofisher.com/ca/en/home/references/ambion-tech-support/rna-isolation/general-articles/the-basics-rna-isolation.html**, (Accessed: 1st June 2020).
14 J. Felbel, *et al.*, Reverse transcription-polymerase chain reaction (RT-PCR) in flow-through micro-reactors: Thermal and fluidic concepts, *Chem. Eng. J.*, 2008, **135**, S298–S302.
15 I. Schneegaß, R. Bräutigam and J. M. Köhler, Miniaturized flow-through PCR with different template types in a silicon chip thermocycler, *Lab Chip*, 2001, **1**, 42–49.
16 A. M. Thompson, *et al.*, Self-Digitization Microfluidic Chip for Absolute Quantification of mRNA in Single Cells, *Anal. Chem.*, 2014, **86**, 12308–12314.
17 J. Liu, M. Enzelberger and S. Quake, A nanoliter rotary device for polymerase chain reaction, *Electrophoresis*, 2002, **23**, 1531–1536.
18 B. H. Park, *et al.*, An integrated rotary microfluidic system with DNA extraction, loop-mediated isothermal amplification, and lateral flow strip based detection for point-of-care pathogen diagnostics, *Biosens. Bioelectron.*, 2017, **91**, 334–340.
19 L. Furuberg, *et al.*, RNA amplification chip with parallel microchannels and droplet positioning using capillary valves, *Microsyst. Technol.*, 2008, **14**, 673–681.
20 J. Wang, *et al.*, SD-chip enabled quantitative detection of HIV RNA using digital nucleic acid sequence-based amplification (dNASBA), *Lab Chip*, 2018, **18**, 3501–3506.
21 E. T. Lagally, I. Medintz and R. A. Mathies, Single-Molecule DNA Amplification and Analysis in an Integrated Microfluidic Device, *Anal. Chem.*, 2001, **73**, 565–570.
22 E. T. Lagally, P. C. Simpson and R. A. Mathies, Monolithic integrated microfluidic DNA amplification and capillary electrophoresis analysis system, *Sens. Actuators, B*, 2000, **63**, 138–146.
23 K. Du, *et al.*, Multiplexed efficient on-chip sample preparation and sensitive amplification-free detection of Ebola virus, *Biosens. Bioelectron.*, 2017, **91**, 489–496.
24 Y. Erh-Chia, *et al.*, Self-powered integrated microfluidic point-of-care low-cost enabling (SIMPLE) chip, *Sci. Adv.*, 2021, **3**, e1501645.
25 I. K. Dimov, *et al.*, Integrated microfluidic tmRNA purification and real-time NASBA device for molecular diagnostics, *Lab Chip*, 2008, **8**, 2071–2078.
26 K. Choi, A. H. C. Ng, R. Fobel and A. R. Wheeler, Digital Microfluidics, *Annu. Rev. Anal. Chem.*, 2012, **5**, 413–440.
27 K. Choi, *et al.*, Automated Digital Microfluidic Platform for Magnetic-Particle-Based Immunoassays with Optimization by Design of Experiments, *Anal. Chem.*, 2013, **85**, 9638–9646.
28 A. H. C. Ng, *et al.*, A digital microfluidic system for serological immunoassays in remote settings, *Sci. Transl. Med.*, 2018, **10**, eaar6076.
29 A. A. Sklavounos, Lab in a Backpack: Portable Digital Microfluidics for Serosurveillance in Resource-Limited Settings, in *Proceedings of the 22nd International Conference on Miniaturized Systems for Chemistry and Life Sciences (μTAS)*, 2018, pp. 164–166.

30 A. Knipes, *et al.*, Use of a rapid digital microfluidics-powered immunoassay for assessing measles and rubella infection and immunity in outbreak settings in the Demographic Republic of the Congo, 2017, Submitted, 2022.
31 B. Coelho, *et al.*, Digital Microfluidics for Nucleic Acid Amplification, *Sensors*, 2017, **17**, 1495.
32 Z. Hua, *et al.*, Multiplexed Real-Time Polymerase Chain Reaction on a Digital Microfluidic Platform, *Anal. Chem.*, 2010, **82**, 2310–2316.
33 M. C. Giuffrida, *et al.*, Isothermal circular-strand-displacement polymerization of DNA and microRNA in digital microfluidic devices, *Anal. Bioanal. Chem.*, 2015, **407**, 1533–1543.
34 D. Decrop, *et al.*, Digital Microfluidics Assisted Sealing of Individual Magnetic Particles in Femtoliter-Sized Reaction Wells for Single-Molecule Detection, in *Microchip Diagnostics*, ed. V. Taly, J. L. Viovy and S. Descroix, Humana Press, New York, NY, 2017, pp. 85–104.
35 B. J. Coelho, *et al.*, A Digital Microfluidics Platform for Loop-Mediated Isothermal Amplification Detection, *Sensors*, 2017, **17**, 2616.
36 M. J. Jebrail, *et al.*, A solvent replenishment solution for managing evaporation of biochemical reactions in air-matrix digital microfluidics devices, *Lab Chip*, 2015, **15**, 151–158.
37 K. Pardee, *et al.*, Paper-Based Synthetic Gene Networks, *Cell*, 2014, **159**, 940–954.
38 K. Pardee, *et al.*, Rapid, Low-Cost Detection of Zika Virus Using Programmable Biomolecular Components, *Cell*, 2016, **165**, 1255–1266.
39 M. Karlikow, *et al.*, Field validation of the performance of paper-based tests for the detection of the Zika and chikungunya viruses in serum samples, *Nat. Biomed. Eng.*, 2022, **6**, 246–256.
40 B. Deiman, P. van Aarle and P. Sillekens, Characteristics and applications of nucleic acid sequence-based amplification (NASBA), *Mol. Biotechnol.*, 2002, **20**, 163–179.
41 I. Swyer, R. Fobel and A. R. Wheeler, Velocity Saturation in Digital Microfluidics, *Langmuir*, 2019, **35**, 5342–5352.
42 Is it possible to determine from the TCID[50] how many plaque forming units to expect?, **https://www.atcc.org/support/technical-support/faqs/converting-tcid-50-to-plaque-forming-units-pfu#:~:text=For any titer expressed as,mean number of PFU%2Fml**, (accessed 25th November 2021).
43 S. J. R. da Silva, *et al.*, Development and Validation of Reverse Transcription Loop-Mediated Isothermal Amplification (RT-LAMP) for Rapid Detection of ZIKV in Mosquito Samples from Brazil, *Sci. Rep.*, 2019, **9**, 4494.
44 D. G. Rackus, *et al.*, Pre-concentration by liquid intake by paper (P-CLIP): a new technique for large volumes and digital microfluidics, *Lab Chip*, 2017, **17**, 2272–2280.
45 J. Zhai, *et al.*, A digital microfluidic system with 3D microstructures for single-cell culture, *Microsyst. Nanoeng.*, 2020, **6**, 6.
46 I. Swyer, *et al.*, Digital microfluidics and nuclear magnetic resonance spectroscopy for in situ diffusion measurements and reaction monitoring, *Lab Chip*, 2019, **19**, 641–653.
47 M. C. Giuffrida and G. Spoto, Integration of isothermal amplification methods in microfluidic devices: Recent advances, *Biosens. Bioelectron.*, 2017, **90**, 174–186.
48 A. A. Sklavounos, C. R. Nemr, S. O. Kelley and A. R. Wheeler, Bacterial Classification and Antibiotic Susceptibility Testing on an Integrated Microfluidic Platform, *Lab Chip*, 2021, **21**, 4208–4222.
49 G. Leone, H. van Schijndel, B. van Gemen, F. R. Kramer and C. D. Schoen, Molecular beacon probes combined with amplification by NASBA enable homogeneous, real-time detection of RNA, *Nucleic Acids Res.*, 1998, **26**, 2150–2155.
50 A. Abd El Wahed, *et al.*, A Portable Reverse Transcription Recombinase Polymerase Amplification Assay for Rapid Detection of Foot-and-Mouth Disease Virus, *PLoS One*, 2013, **8**, e71642.
51 I. M. Lobato and C. K. O'Sullivan, Recombinase polymerase amplification: Basics, applications and recent advances, *TrAC, Trends Anal. Chem.*, 2018, **98**, 19–35.
52 M. M. Ali, *et al.*, Rolling circle amplification: a versatile tool for chemical biology{,} materials science and medicine, *Chem. Soc. Rev.*, 2014, **43**, 3324–3341.
53 Q. Vo and T. Tran, Droplet ejection by electrowetting actuation, *Appl. Phys. Lett.*, 2021, **118**, 161603.
54 ZIKV-001: Infection of three rhesus macaques with French Polynesian Zika virus, **https://zika.labkey.com/project/OConnor/ZIKV-001/begin.view**, (accessed 1st June 2020).
55 A. Sklavounos, *et al.*, Digital Microfluidic Hemagglutination Assays for Blood Typing, Donor Compatibility Testing, and Hematocrit Analysis, *Clin. Chem.*, 2021, **67**, 1699–1708.
56 S. Anderson, B. Hadwen and C. Brown, Thin-film-transistor digital microfluidics for high value in vitro diagnostics at the point of need, *Lab Chip*, 2021, **21**, 962.
57 S. von der Ecken, A. A. Sklavounos and A. R. Wheeler, Vertical Addressing of 1-Plane Electrodes for Digital Microfluidics, *Adv. Mater. Technol.*, 2021, DOI: **10.1002/admt.202101251**, in press.
58 J. H. Smith, D. H. Persing, A. Wortman, R. Chang and D. Swenson, Methods and apparatus for sequential amplification reactions, *US Pat.*, 8900828B2, 2014.
59 Meridian Bioscience, Revogene, **https://www.meridianbioscience.com/diagnostics/platforms/molecular/revogene/?country=CA**, (accessed 25th January 2022).
60 E. Trullols, I. Ruisánchez and F. X. Rius, Validation of qualitative analytical methods, *TrAC, Trends Anal. Chem.*, 2004, **23**, 137–145.
61 A. Ríos, *et al.*, Quality assurance of qualitative analysis in the framework of the European project 'MEQUALAN', *Accredit. Qual. Assur.*, 2003, **8**, 68–77.
62 C. M. Florkowski, Sensitivity, specificity, receiver-operating characteristic (ROC) curves and likelihood ratios:

communicating the performance of diagnostic tests, *Clin. Biochem. Rev.*, 2008, **29**(Suppl 1), S83–S87.

63 E. K. Heiniger, *et al.*, Comparison of point-of-care-compatible lysis methods for bacteria and viruses, *J. Microbiol. Methods*, 2016, **128**, 80–87.

64 A. M. Bingham, *et al.*, Comparison of Test Results for Zika Virus RNA in Urine, Serum, and Saliva Specimens from Persons with Travel-Associated Zika Virus Disease — Florida, 2016, *Morb. Mortal. Wkly. Rep.*, 2016, **65**, 475–478.